

Static and Dynamic Stereochemistry of *N*-(1,4-Dimethyl-9-triptycyl)-hydroxylamine Derivatives

Gaku Yamamoto,* Chiharu Agawa, Takahiro Ohno, Mao Minoura, and Yasuhiro Mazaki

Department of Chemistry, School of Science, Kitasato University, Kitasato, Sagami-hara, Kanagawa 228-8555

Received March 18, 2003; E-mail: gyama@kitasato-u.ac.jp

Static and dynamic stereochemistry of *N*-alkyl, *O*-alkyl, and *N,O*-dialkyl derivatives of *N*-(1,4-dimethyl-9-triptycyl)hydroxylamine were studied. X-ray crystallographic analysis revealed that an *N*-alkyl derivative adopts $R^*(-sc)^*$ conformation while *N,O*-dialkyl derivatives adopt R^*-ap conformation. In solution, stereomutation was almost frozen on the NMR timescale at ca. -60°C . The same conformer as found in the crystal was the major conformer in solution in each compound, and a small amount of a second conformer was found in equilibrium with the major one for the *N*-alkyl and *N,O*-dialkyl derivatives. The stereomutation was interpreted in terms of diastereomerization and enantiomerization, and the ^1H NMR lineshape analysis afforded the activation parameters for these processes.

We recently reported the static and dynamic stereochemistry of several *N*-alkyl and *N,O*-dialkyl derivatives of *N*-9-triptycylhydroxylamine (**1a**) such as **1b–1d**,¹ and of some *O*-alkyl derivatives such as **1e** (Chart 1).² X-ray crystallographic analysis of these compounds revealed that the nitrogen atom is pyramidal and the molecule adopts a chiral conformation. Dynamic NMR studies in solution showed that the stereomutation by which the chiral conformation enantiomerizes takes place rapidly at room temperature but slows down at low temperatures. For the *N*-alkyl and *N,O*-dialkyl derivatives, the stereomutation was interpreted in terms of two rate processes: “R-passing” and “O-passing”, in which the alkyl group R or the oxy group OR', respectively, passes over a benzene ring of the 9-triptycyl (Tp) moiety.¹ Either process is accompanied by inversion of the nitrogen atom and partial rotation of the N–O bond, but the energy barrier is mainly governed by the steric repulsion among the substituents around the N–O moiety rather than the intrinsic barriers to the nitrogen inversion and the N–O bond rotation. Thus the Tp–N rotation is always accompanied by chirality reversal in these compounds.

On the other hand, in the *O*-alkyl derivatives carrying a hydrogen atom on the nitrogen such as **1e**, the rotation around the Tp–N bond with retaining the chirality had a lower energy barrier than the chirality reversal.²

We planned to extend these studies to derivatives of **1a** carrying a substituent at a peri position of the triptycene skeleton. In such derivatives, the presence of conformational diastereomers is expected and the effects of the peri substituent on the conformational equilibria and on the conformational interconversion will be of interest. We report here the static and dynamic stereochemistry of *N*-(1,4-dimethyl-9-triptycyl)hydroxylamine derivatives **2–8** (Chart 1). The 4-methyl group was introduced solely because of the synthetic convenience.

Results and Discussion

Synthesis. Compounds **2–8** were synthesized as shown in Scheme 1. 9-Nitroanthracene was treated with 3,6-dimethyl-benzenediazonium-2-carboxylate, which was prepared in situ by diazotization of 3,6-dimethylantranilic acid,³ to afford 1,4-dimethyl-9-nitrotriptycene (**9**) together with a considerable amount of the corresponding 1,4-adduct, 5,12-dihydro-1,4-dimethyl-6-nitro-5,12-ethenonaphthacene (**10**). Reduction of **9** with lithium tetrahydridoaluminate gave *N*-(1,4-dimethyl-9-triptycyl)hydroxylamine (**11**). Reaction of **11** with KO^tBu followed by methyl and ethyl iodides afforded the *O*-alkyl compounds **2** and **3**, respectively. Meanwhile, reaction of **11** with methyl trifluoromethanesulfonate (triflate) gave the *N*-methyl compound **4**, which was then *O*-alkylated by treating first with KO^tBu, then with methyl and ethyl triflates, to afford **5** and **6**, respectively. The corresponding iodides instead of the triflates gave similar results in the *O*-alkylation. Direct *N*-ethylation of **11** with ethyl triflate, however, was by no means successful, presumably because of steric hindrance. Treatment of **2** and **3** with BuLi followed by C₂H₅I afforded the *N*-ethyl compounds **7** and **8**, respectively.

Preliminary Conformational Analysis. The most stable conformation of hydroxylamine and its simple alkyl deriva-

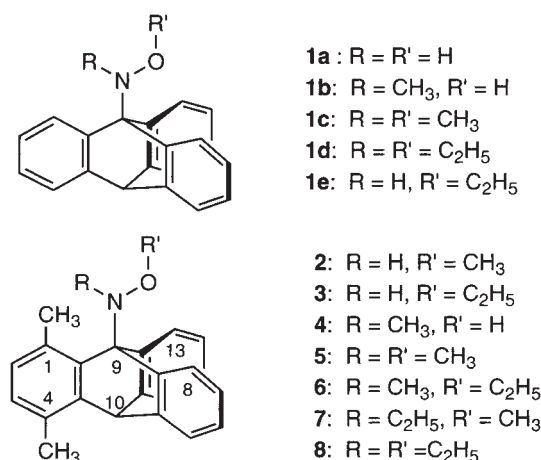
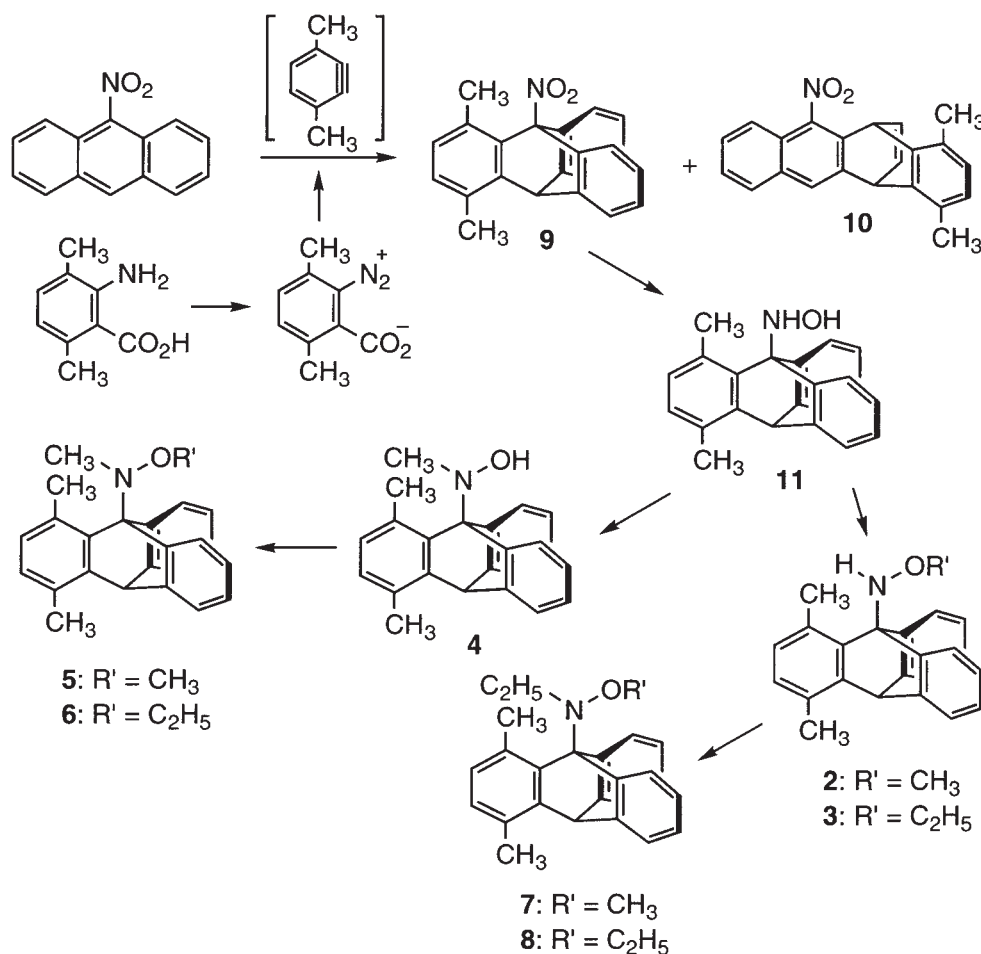
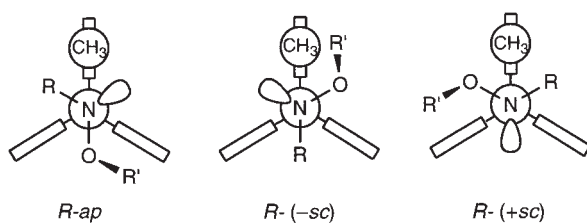


Chart 1.



Scheme 1.



Scheme 2.

tives has been deduced to be as follows: the nitrogen is pyramidal and the *O*-substituent is eclipsed with the nitrogen lone-pair and is thus anticlinal to the *N*-substituents.⁴ Based on this assumption together with the results on the *N*-9-triptycylhydroxylamines **1** reported previously,^{1,2} three diastereomeric conformers are assumed for the present compounds, each of which is chiral and consists of a pair of enantiomers (Scheme 2). These diastereomeric conformers are named as *R**-*ap*, *R**-(-*sc*)*, and *R**-(+*sc*)*. Here, *R*/*S* refers to the absolute configuration of the nitrogen atom and *ap*/+*sc*/-*sc* refers to the absolute configuration around the Tp-N bond; *R**-(-*sc*)* denotes either *R*-(-*sc*) or its enantiomer *S*-(+*sc*), or a racemic mixture of both.⁵

The relative abundance of these diastereomeric conformers naturally depends on the nature of the substituents *R* and *R*', as discussed in detail in the following sections. A priori, the *R**-

(+*sc*)* isomer is thought to be least stable because the close proximity of the *R* and *OR*' groups to the 1-methyl group will cause significant steric repulsion.

X-ray Crystallography. Single crystals suitable for X-ray analysis were obtained for compounds **4–7** and were subjected to X-ray crystallographic analysis. The perspective drawings of the molecular structures of **4–7** are shown in Fig. 1 and the representative bond lengths and angles are compiled in Table 1.

In any of the compounds, the nitrogen atom is pyramidal; the sum of the bond angles around the nitrogen atom is 326–327° compared with 328.4° for the tetrahedral geometry. The Tp-N bond is almost perfectly staggered; the C1-N-O plane (see numbering in Table 1) almost bisects the planes of the two flanking benzene rings of the triptycene moiety. These features were previously found in *N,O*-diethyl-*N*-9-triptycylhydroxylamine (**1d**).¹ The *N*-methyl group of compound **4** is located between the two peri-unsubstituted benzene rings, and the OH group is flanked by the 1-methyl group, thus the molecule adopts the *R**-(-*sc*)* conformation (Scheme 2). Although the crystal of **4** was disordered by the presence of the enantiomers in a ratio of 69:31, the presence of the diastereomers was not observed. On the contrary, in the *N,O*-dialkyl compounds **5–7**, the alkoxy group is located between the two peri-unsubstituted benzene rings and the *N*-alkyl group is flanked by the 1-methyl group; thus the molecules adopt

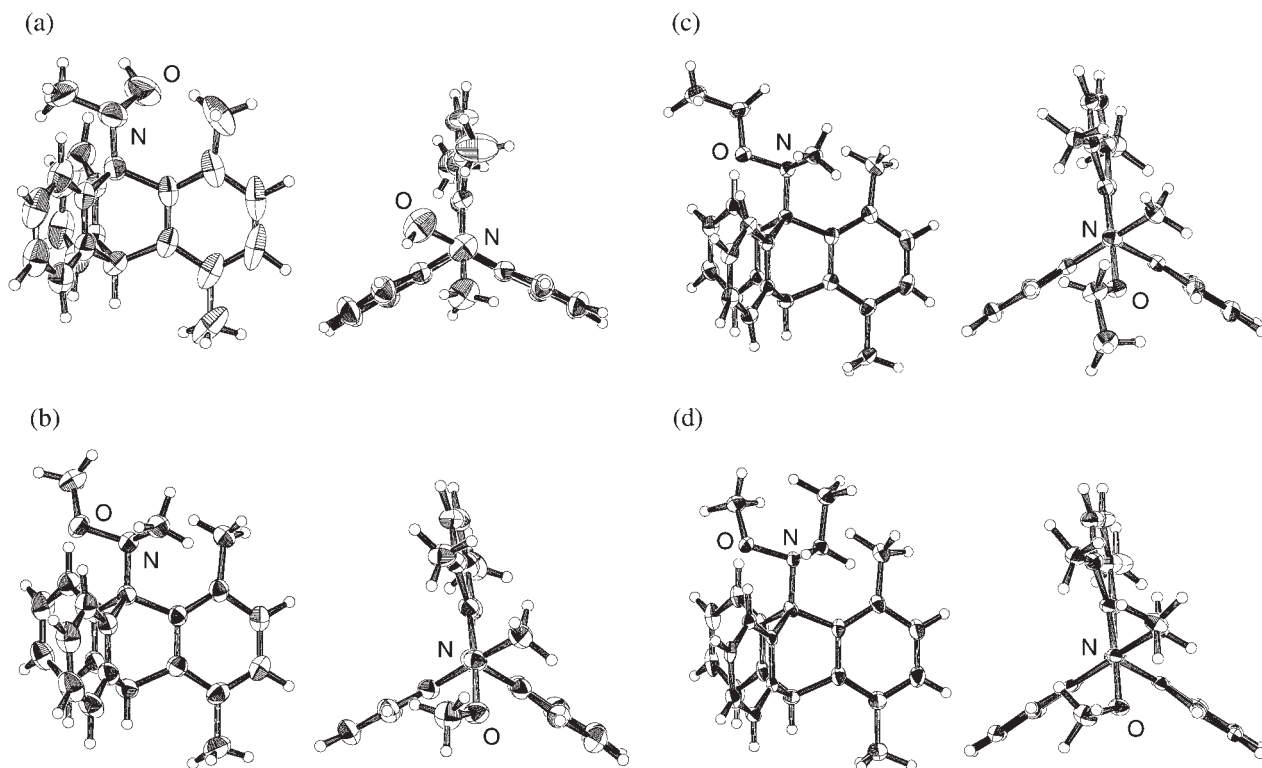


Fig. 1. Side and top views of the X-ray molecular structures of (a) compound **4**, (b) compound **5**, (c) compound **6**, and (d) compound **7**.

the R^* -*ap* conformation. This remarkable contrast between the *N*-alkyl and the *N,O*-dialkyl compounds will be discussed in a later section.

The C1–N–O–C9 dihedral angles (see numbering in Table 1) in **5–7** range 136° to 155°; such values are similar to those found in **1d**¹ and **1e**² (148 and 151°, respectively). The deviation from the intrinsic value of 120° may be mainly due to the steric interaction of the alkyl group on the oxygen with the tryptene skeleton, as discussed previously.^{1,2}

Stable Conformers of the *O*-Alkyl Derivatives in Solution. In the ¹H and ¹³CNMR, the *O*-alkyl compounds **2** and **3** carrying a hydrogen atom on the nitrogen gave fast-exchange-limit spectra at ambient temperature, all the signals being averaged over conformers. Upon lowering the temperature in CD₂Cl₂, the two peri-unsubstituted benzene rings became nonequivalent: the signal at the lowest field of the aromatic region (δ ca. 7.7), which appeared as a sharp doublet at 23 °C and was assigned to 8/13-H, broadened, decoalesced into two signals at ca. –20 °C and appeared as two sharp equally intense doublets at ca. δ 7.6 and 7.8 at –60 °C for both compounds. In concert with this lineshape change of the aromatic signals, the *O*-methylene signal of **3**, which appeared as a quartet at δ 4.25 at 23 °C, also broadened and decoalesced into a complex multiplet ascribed to the AB part of the ABX₃ spin system upon lowering the temperature. Throughout the temperature range examined, the 1-methyl and 4-methyl signals each remained a sharp singlet.

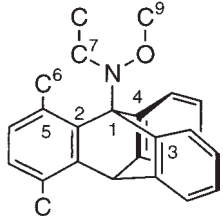
The identity of the conformers was inferred by the nuclear Overhauser effect (NOE) experiments at ca. –60 °C. For the *O*-ethyl compound **3**, irradiation of the 1-methyl signal at δ 2.65 enhanced the NH signal at δ 7.28. Irradiation of the

methylene signal at δ 4.27 enhanced the higher-field one of the peri-proton signals at δ 7.59, while irradiation of the lower-field one of the peri-proton signals at δ 7.83 enhanced the NH signal. Although these NOE data are compatible with both the R^* -*ap* and R^* -(+sc)* conformers, the former is more reasonable because of the steric congestion of the latter.

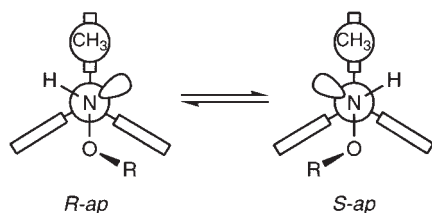
These findings thus suggested that the *O*-alkyl compounds **2** and **3** reside in a single diastereomeric conformer R^* -*ap* and that the lineshape changes are caused by the interconversion between the two enantiomeric conformers R -*ap* and S -*ap* shown in Scheme 3.

Stable Conformers of the *N*-Alkyl and *N,O*-Dialkyl Derivatives in Solution. The *N*-methyl compound **4** and the *N,O*-dialkyl compounds **5–8** behaved somewhat differently from the *O*-alkyl compounds **2** and **3** mentioned above. In the ¹H NMR spectra at 23 °C, the 1- and 4-methyl groups as well as the *N*- and *O*-methyl groups gave a single signal for each, some being broadened, while the two peri-unsubstituted benzene rings were nonequivalent and the methylene protons of the *N*- and *O*-ethyl groups were also anisochronous, although the signals were broadened. When the temperature was lowered, the aromatic and methylene signals became sharp and each of the methyl signals split into two unequally intense singlets, indicating the presence of two diastereomeric conformers and the slowing-down of the interconversion between them on the NMR timescale.

In the *N*-methyl compound **4**, the signal integration showed the presence of two conformers in a ratio of 87:13 at –60 °C (Table 2). Irradiation of the *N*-methyl protons of the major conformer at δ 3.75 enhanced two aromatic signals at δ 7.47 and 8.28 ascribable to 8-H and 13-H, clearly indicating that

Table 1. Representative Bond Lengths (Å) and Angles (°) for Compounds **4–7**^{a)}


Compound	4	5	6	7
N–O	1.497(3)	1.461(2)	1.460(2)	1.475(2)
N–C1	1.463(2)	1.468(2)	1.469(3)	1.480(2)
N–C7	1.482(3)	1.482(2)	1.472(3)	1.492(2)
O–C9	—	1.422(2)	1.426(3)	1.424(2)
C1–C2	1.566(2)	1.568(2)	1.571(3)	1.561(2)
C1–C3	1.547(2)	1.544(2)	1.540(3)	1.548(2)
C1–C4	1.535(2)	1.558(2)	1.566(3)	1.559(2)
O–N–C1	107.7(2)	107.0(2)	106.8(2)	106.2(1)
O–N–C7	105.3(2)	106.4(2)	106.0(2)	106.9(1)
C1–N–C7	113.3(2)	113.8(2)	113.2(2)	112.8(1)
N–O–C9	—	108.1(2)	108.4(2)	110.7(1)
N–C1–C2	115.0(2)	111.1(2)	111.2(2)	111.0(1)
N–C1–C3	114.3(2)	114.0(2)	113.8(2)	114.9(1)
N–C1–C4	111.5(2)	115.7(2)	115.4(2)	115.5(1)
C1–C2–C5	128.9(2)	128.8(2)	129.5(2)	128.7(2)
C2–C5–C6	126.0(3)	127.6(2)	127.1(2)	126.8(2)
C1–N–O–C9	—	−145.5(2)	−154.5(2)	−136.2(1)
O–N–C1–C2	65.0(2)	174.8(2)	177.4(2)	176.3(1)
O–N–C1–C3	−56.9(2)	60.8(2)	62.2(2)	62.1(2)
O–N–C1–C4	−178.7(2)	−60.1(2)	−58.6(2)	−58.7(2)
C7–N–C1–C2	—	−68.0(2)	−66.4(2)	−66.9(2)
C7–N–C1–C3	—	178.0(2)	178.5(2)	178.9(1)
C7–N–C1–C4	—	57.1(2)	57.7(3)	58.1(2)
N–C1–C2–C5	4.3(3)	−12.3(2)	−11.9(3)	−12.7(2)
C1–C2–C5–C6	8.0(4)	−1.9(3)	−5.8(4)	−8.0(3)

a) Dihedral angles are for the molecules with the *S* configuration at the nitrogen atom.

Scheme 3.

the *N*-methyl group is located between the two peri-unsubstituted benzene rings and thus the major conformer is *R*[∗]-(−*sc*)[∗], that is the one found in the crystalline state as mentioned above. Irradiation of the 1-methyl protons at δ 2.82 enhanced the OH signal at δ 6.19, suggesting that the OH proton is located close to the 1-methyl group. Although the structure of the minor conformer could not be experimentally determined, *R*[∗]-*ap* is reasonably assigned because *R*[∗]-(+*sc*)[∗] will be highly disfavored due to the steric congestion.

In the *N,O*-dimethyl compound **5**, two conformers were present at −60 °C in a ratio of ca. 95:5. The results of

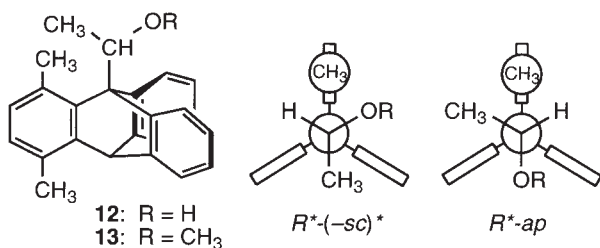
NOE experiments together with the steric considerations indicated that the major conformer was *R*[∗]-*ap*: irradiation of the *N*-methyl protons enhanced one peri-proton signal at δ 8.22 as well as the 1-methyl signal at δ 2.68, while irradiation of the *O*-methyl protons at δ 4.04 enhanced the other peri-proton signal at δ 7.56. Therefore the major conformer in solution is again the one found in the crystal. The minor conformer is assumed to be *R*[∗]-(−*sc*)[∗], based on the steric considerations.

Reversal of the major conformer on going from the *N*-hydroxy compound **4** to the *N*-alkoxy compounds **5–8** and the predominance of *R*[∗]-*ap* in the latter compounds are noteworthy. We previously reported that in 9-(1-hydroxyethyl)-1,4-dimethyltriptycene (**12**) and 9-(1-methoxyethyl)-1,4-dimethyltriptycene (**13**), the carbon analogs of **4** and **5**, respectively, rotation of the bridgehead-to-substituent bond was slow on the NMR time scale at room temperature, and two conformers, *R*[∗]-(−*sc*)[∗] and *R*[∗]-*ap*, were found at equilibrium (Scheme 4).^{6,7} In either compound the *R*[∗]-(−*sc*)[∗] form was predominant, and the ratio of the two conformers in CDCl₃ at 23 °C was 86:14 for **12** and 78:22 for **13**. The results were interpreted as natural, because it is generally accepted that a hydroxy or

Table 2. Conformer Populations and Energy Barriers to Stereomutation

Compd	R	R'	Pop ^{a)}	Free energy of activation ^{b)}	
				Diastereomerization ^{c)}	Enantiomerization
2	H	Me	~100	— ^{d)}	52.3 (250 K)
3	H	Et	~100	— ^{d)}	52.4 (250 K)
4	Me	H	15	53.2; 49.6 (250 K)	76.9 (350 K) ^{e)}
5	Me	Me	95	— ^{d)}	71.0 (350 K) ^{e)}
6	Me	Et	>96	— ^{d)}	72.0 (350 K) ^{e)}
7	Et	Me	73	57.8; 59.9 (250 K)	64.7 (320 K)
8	Et	Et	70	55.8; 57.5 (250 K)	— ^{f)}

a) Population (%) of R^* -ap in CDCl_3 at ca. -60°C , which is almost independent of the temperature. b) Measured in CDCl_3 unless otherwise stated. Given in kJ mol^{-1} at temperatures in parentheses and reliable to $\pm 0.4 \text{ kJ mol}^{-1}$. c) The former value is for the $R^*(-sc)^* \rightarrow R^*$ -ap process and the latter for the reverse process. d) Not obtained because the diastereomer equilibrium is too one-sided. e) Measured in toluene- d_8 . f) Not obtained because the NMR lineshape change is too complex.



Scheme 4.

methoxy group is less bulky than a methyl group,⁸ and the $R^*(-sc)^*$ form is sterically more favored. If the entropy difference between the conformers is neglected, the conformer ratio at -60°C is calculated to be 93:7 for **12** and 86:14 for **13**, respectively.

The different behavior for the hydroxylamine **5** and for the ether **13** will be understood as follows. As discussed in detail in the previous paper,¹ the N–O bond in a hydroxylamine prefers a conformation where the *N*- and *O*-alkyl groups arrange anticlinal (120°) to each other, mainly because of the electrostatic interaction between the lone-pair electrons on the N and O atoms, while in an ether the corresponding C–O bond prefers a staggered conformation where the alkyl groups on the C and O atoms are synclinal (60°) or antiperiplanar (180°) to each other. Furthermore, the rotational barrier around the N–O bond is higher than that around the C–O bond. Because of these factors, the steric repulsion between the 1-methyl group and the *O*-methyl group (or more strictly the OCH_3 moiety) in the $R^*(-sc)^*$ form will be severer in **5** than in **13**. Therefore, in compound **5**, the steric interaction of the 1-methyl group with the methoxy group can be larger than that with the *N*-methyl group, and the R^* -ap conformer can be predominant, which is actually observed.

In the hydroxy compounds **4** and **12**, a small steric demand of the OH hydrogen does not cause serious steric interaction with the 1-methyl group and thus results in similar conformer distributions between **4** and **12** (95:5 vs 97:3 at -60°C).

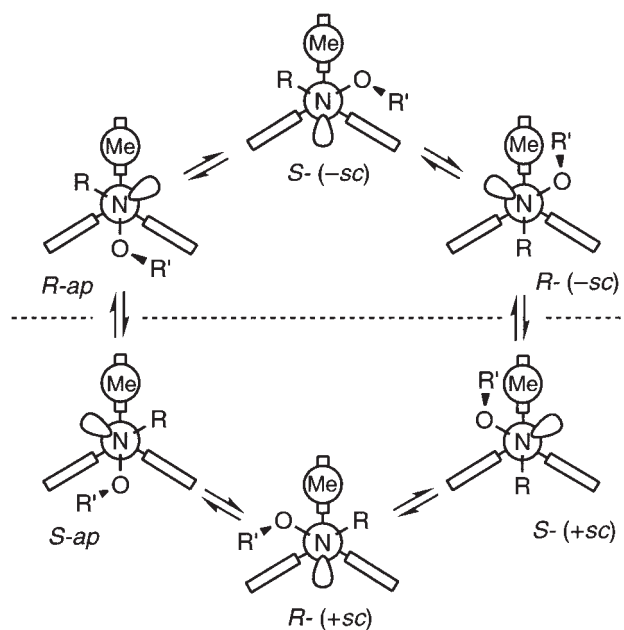
In compound **6**, the conformational equilibrium was again

overwhelmingly inclined to R^* -ap ($>96\%$); the NMR signals of the minor isomer were detected but a reliable determination of the populations could not be made. The similar conformational preferences in **5** and **6** will be reasonable because the *O*-ethyl group in **6** would exert similar steric effects toward the other part of the molecule as the *O*-methyl group in **5**.

In the *N*-ethyl compounds **7** and **8**, two diastereomeric conformers were found at -60°C ; NOE experiments confirmed that the major isomer is R^* -ap. The population of this isomer was 73% and 70% for **7** and **8**, respectively. The smaller proportion of this form relative to the *N*-methyl compounds **5** and **6** will be ascribed to the larger steric interaction of the *N*-ethyl group with the 1-methyl group in **7** and **8** than that of the *N*-methyl group in **5** and **6**.

Conformational Interconversion. The plausible itinerary of the conformational interconversion in the compounds examined is shown in Scheme 5. One conformer moves into a neighboring one by passing of either the alkyl group R or the oxy group OR' over a benzene ring of the triptycene moiety, which is accompanied by inversion of the nitrogen and partial rotation of the N–O bond. Rotation of the triptycene–nitrogen bond without the nitrogen inversion is deduced to have a far higher energy barrier than the processes given in Scheme 5, as previously discussed in detail,^{1,2} and this possibility is not considered in the following discussion.

For compounds **2** and **3**, only a single diastereomer R^* -ap was observed, as discussed in the former section. The peripron (8/13-H) signals of these compounds appeared as two equally intense doublets at low temperatures, which coalesced into a single doublet upon elevation of the temperature, reflecting the increase in the enantiomerization rate. Figure 2 shows the spectra at various temperatures for compound **2**. Total lineshape analysis afforded the rate constants for the enantiomerization at temperatures below 0°C (Fig. 2, right), from which the Eyring parameters ΔH^\ddagger and ΔS^\ddagger were obtained by the least squares treatments (Table 4 in the Experimental



Scheme 5.

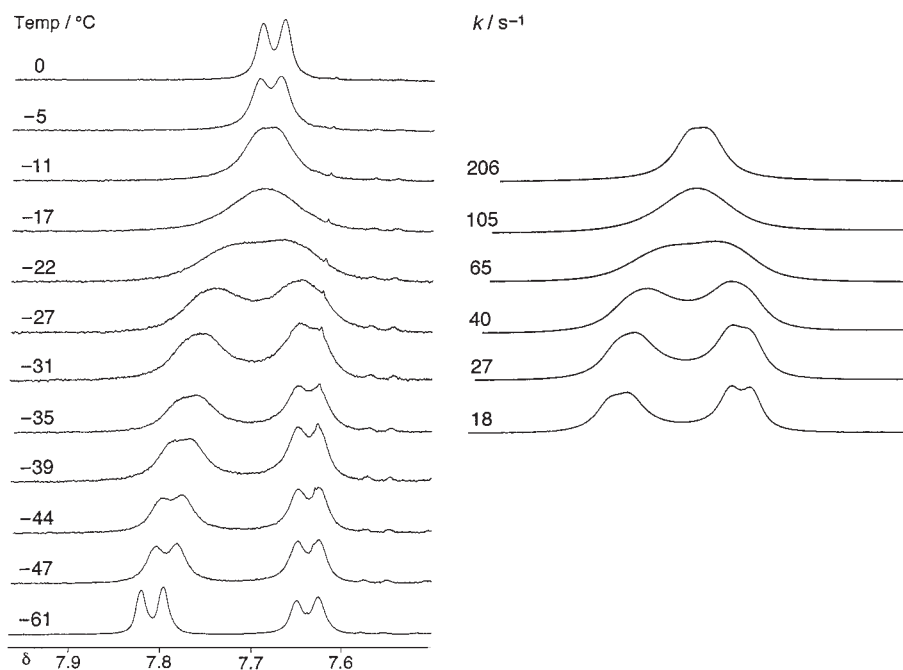


Fig. 2. The observed spectra of the peri-proton region of compound **2** in CDCl_3 at various temperatures (left) and the calculated spectra with the best-fit rate constants (right).

Section). The free energies of activation ΔG^\ddagger at 250 K were calculated from these values to be 52.3 and 52.4 kJ mol^{-1} for **2** and **3**, respectively (Table 2). The lineshape analysis of the *O*-methylene signals of **3** gave the value of 52.3 kJ mol^{-1} , which is in accordance with the data from the peri-proton analysis.

The conformational interconversion between *R*-*ap* and *S*-*ap* in compounds **2** and **3** will reasonably occur directly by the passing of *N*-H over the 1-methyl group accompanied by nitrogen inversion and partial rotation of the *N*-O bond; thus the roundabout pathway by way of the four unstable conformers, $R^*-(+sc)^*$ and $R^*(-sc)^*$, in Scheme 5 will be less likely.

For compounds **4–8**, interconversion among the conformers is frozen on the NMR timescale at -60°C and the two diastereomeric conformers are separately observed, the population of the $R^*-(+sc)^*$ form being undetectably small. Interconversion between *R*-(*sc*) and *R*-*ap* in the upper half of Scheme 5, for example, takes place by the successive passing of the *N*-alkyl and *N*-oxy groups over the peri-unsubstituted benzene rings of the triptycene skeleton (“*R*-passing” and “*O*-passing”, respectively) by way of *S*-(*sc*) with concomitant nitrogen inversion and partial rotation of the *N*-O bond in each step. When this diastereomerization process is fast on the NMR timescale, the NMR signals of the 1- and 4-methyl groups as well as of other methyl groups in the *N*- and *O*-alkyl moieties are averaged among conformers but the two methylene protons in an *N*- or *O*-ethyl group still remain diastereotopic and thus anisochronous, and the two peri-unsubstituted benzene rings are nonequivalent.

Interconversion between the conformers in the upper and lower halves in Scheme 5, which may be referred to as “enantiomerization”, requires the passing of the *N*-alkyl or *N*-oxy group over the benzene ring carrying the 1-methyl group, and will have a higher energy barrier than the diastereomerization processes. When this process becomes fast on the NMR

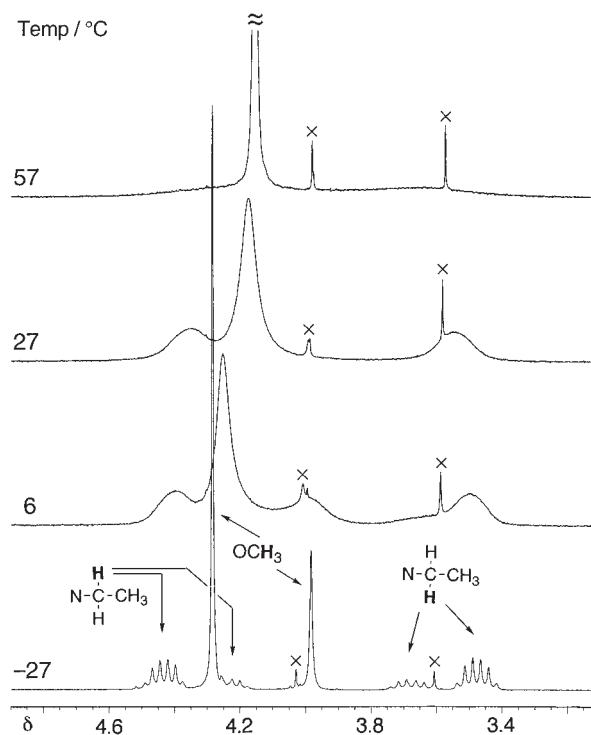


Fig. 3. The temperature dependence of the *O*-methyl and *N*-methylene signals of compound **7** in CDCl_3 . Peaks marked with \times are due to impurities.

timescale, the methylene protons become isochronous and the two peri-unsubstituted benzene rings become equivalent.

As a typical example, the temperature dependence of the spectrum of compound **7** is shown in Fig. 3. At -27°C , both the diastereomerization and the enantiomerization are slow;

two singlets for the OCH₃ protons and two pairs of multiplets for the methylene protons are observed. At 6 °C, two singlets, two high-field multiplets, and two low-field multiplets are going to mutually coalesce. At 27 °C three broad peaks are observed: the OCH₃ signal appears as a single broad peak while the methylene signals appear as two broad peaks, indicating that the diastereomerization is fast but the enantiomerization is still slow on the NMR timescale. At 57 °C the two methylene signals are going to coalesce.

For the *N*-methyl derivative **4**, the lineshape analysis of the 1-methyl signals in the range of −52 to −22 °C in CDCl₃ gave the $\Delta G^\ddagger = 53.1 \text{ kJ mol}^{-1}$ at 250 K for the $R^*(-sc)^* \rightarrow R^*-ap$ diastereomerization process, while that of the 8-H and 13-H signals in the range of 80 to 117 °C in toluene-*d*₈ gave the $\Delta G^\ddagger = 76.9 \text{ kJ mol}^{-1}$ at 350 K for the enantiomerization process.

For compounds **5** and **6**, the energy barrier to the diastereomerization process could not be obtained because the diastereomer equilibrium was strongly biased to R^*-ap . The lineshape analysis of the 8-H and 13-H signals in toluene-*d*₈ gave the enantiomerization barrier of $\Delta G^\ddagger = 71.0$ and 72.0 kJ mol^{-1} at 350 K for **5** and **6**, respectively.

For compounds **7** and **8**, the lineshape analysis of the 1-methyl signal in CDCl₃ (see Fig. 4 for **7**) afforded the $R^*(-sc)^* \rightarrow R^*-ap$ barrier; $\Delta G^\ddagger = 57.8$ and 55.8 kJ mol^{-1} at 250 K for **7** and **8**, respectively. The lineshape analysis of the methylene signals of **7** (see Fig. 5) afforded the enantiomerization barrier; $\Delta G^\ddagger = 64.7 \text{ kJ mol}^{-1}$ at 320 K. For compound **8**, the lineshape change of the methylene signals as well as of the peri-proton signals was too complex to analyze because of the signal overlap, and the analysis was abandoned.

The energy barriers to stereomutation thus obtained are compiled in Table 2. That the diastereomerization barrier in

7 and **8** is higher than that in **4** will be easily understood in terms of the larger steric repulsion at the transition states in the former compounds, even without considering which of the R-passing and the O-passing is the rate-determining step (It has been deduced that the former has a higher barrier in compounds **1**¹).

The decrease in the enantiomerization barrier on going from **4** to **5** or **6**, and on going from **5** to **7** is remarkable. Here again there are two possibilities of enantiomerization routes: R-passing ($R-ap \rightleftharpoons S-ap$) and O-passing [$R(-sc) \rightleftharpoons S(+sc)$]; the former will have a higher barrier than the latter if the steric congestion around the 1-methyl group at the transition states is considered. If we assume that the O-passing is the preferred path, the energy barrier trend, **4** > **5** ~ **6** > **7**, can not be understood simply in terms of the steric congestion at the transition states, and should be ascribed, at least partly, to the larger destabilization of the ground state by a bulkier group.

Experimental

General. Melting points are not corrected. ¹H and ¹³C NMR spectra were obtained on a Bruker ARX-300 spectrometer operating at 300.1 MHz for ¹H and 75.4 MHz for ¹³C, respectively, at 22–23 °C, unless otherwise stated. Chemical shifts were referenced with internal tetramethylsilane ($\delta_H = 0$) or CDCl₃ ($\delta_C = 77.0$). Letters p, s, t, and q given with the ¹³C chemical shifts denote primary, secondary, tertiary, and quaternary, respectively. In variable-temperature experiments, temperatures were calibrated using a methanol sample or an ethylene glycol sample and are reliable to ± 1 °C.

1,4-Dimethyl-9-nitrotriptcene (9). To a boiling solution of 1.79 g (8.0 mmol) of 9-nitroanthracene in 25 mL of butanone was added simultaneously 3.96 g (24.0 mmol) of 3,6-dimethylantranilic acid³ in 100 mL of butanone and 6.45 mL (48.0 mmol) of

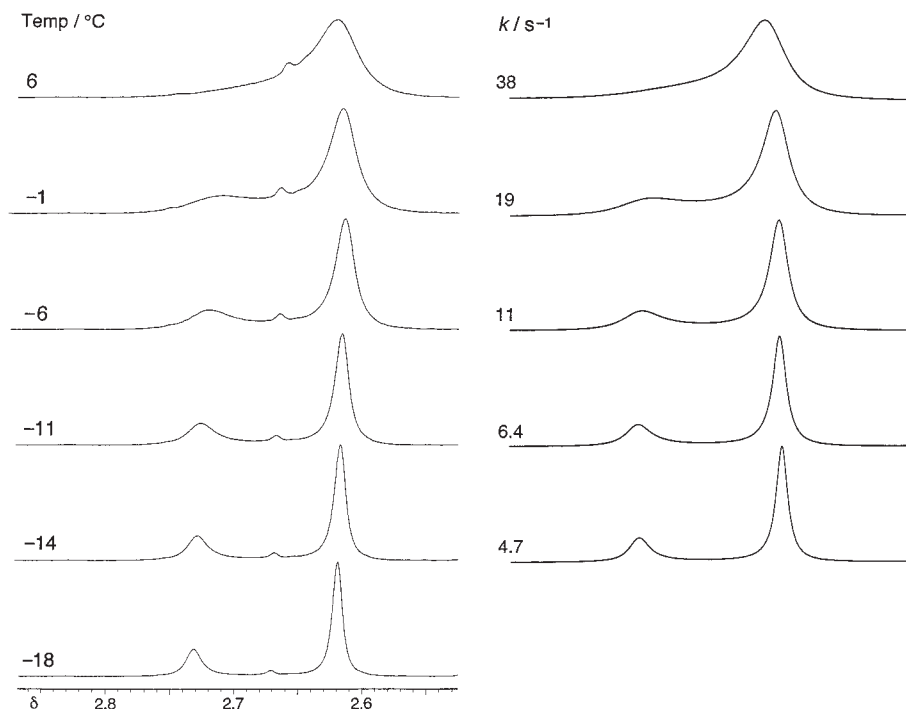


Fig. 4. The observed spectra of the 1-methyl signals of compound **7** in CDCl₃ at various temperatures (left) and the calculated spectra with the best-fit rate constants for the diastereomer interconversion (right).

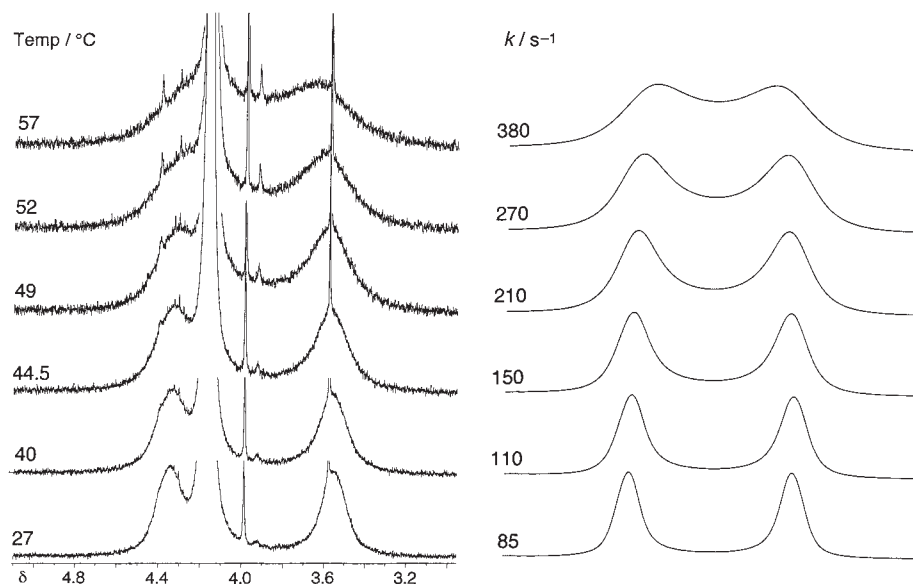


Fig. 5. The observed spectra of the methylene signals of compound **7** in CDCl_3 at various temperatures (left) and the calculated spectra with the best-fit rate constants for the enantiomer interconversion (right). The large signal at δ ca. 4.2 is due to the OCH_3 protons, and the other small sharp signals are due to impurities.

isopentyl nitrite in 100 mL of butanone during a course of 5 h, and the mixture was heated under reflux for 1 h. The ^1H NMR spectrum of the reaction mixture revealed the presence of 9-nitroanthracene, the desired 9,10-adduct **9**, and the 1,4-adduct **10** in a ratio of 8:10:7. After evaporation of the solvent and dissolution of the residue to 25 mL of butanone, the same procedure as above was repeated, affording a 4:10:7 mixture. Column chromatography on alumina with hexane–dichloromethane as the eluent, followed by recrystallization from dichloromethane–hexane, afforded 0.78 g (2.38 mmol, 30%) of **9**, mp 246–248 °C. Found: C, 80.86; H, 5.28; N, 4.32%. Calcd for $\text{C}_{22}\text{H}_{17}\text{NO}_2$: C, 80.71; H, 5.23; N, 4.28 %. ^1H NMR (CDCl_3) δ 2.294 (3H, s), 2.506 (3H, s), 5.594 (1H, s), 6.738 (1H, d, $J = 7.9$ Hz), 6.836 (1H, d, $J = 7.9$ Hz), 7.05–7.15 (4H, m), 7.395 (2H, m), 7.915 (2H, m). ^{13}C NMR (CDCl_3) δ 18.07 (1C, p), 18.72 (1C, p), 50.50 (1C, t), 95.69 (1C, q), 122.76 (2C, t), 123.31 (2C, t), 125.57 (2C, t), 126.55 (2C, t), 127.99 (1C, t), 129.68 (1C, q), 129.71 (1C, t), 130.09 (1C, q), 138.81 (1C, q), 140.72 (2C, q), 141.56 (1C, q), 143.84 (2C, q).

The 1,4-adduct **10** was identified by ^1H NMR (CDCl_3): δ 2.45 (3H, s), 2.47 (3H, s), 5.52 (1H, dd, $J = 6.0$ and 1.6 Hz), 5.73 (1H, dd, $J = 6.2$ and 1.5 Hz), 6.78 (2H, s), 6.95 (1H, m), 7.4–7.6 (3H, m), 7.7–7.8 (3H, m).

***N*-(1,4-Dimethyl-9-triptycyl)hydroxylamine (11).** To an ice-cold solution of 0.98 g (3.0 mmol) of **9** in 200 mL of dry diethyl ether was added under argon atmosphere 0.455 g (12 mmol) of lithium tetrahydridoaluminate, and the mixture was stirred for 2.5 h at room temperature and quenched with water. The mixture was washed successively with aq NaHCO_3 , water, and brine, and dried over MgSO_4 . After evaporation of the solvent, the residue was recrystallized from dichloromethane–hexane (3:2) to afford 0.82 g (2.6 mmol, 87%) of **11** as colorless crystals, mp 219–221 °C. Found: C, 84.57; H, 6.06; N, 4.47%. Calcd for $\text{C}_{22}\text{H}_{19}\text{NO}$: C, 84.32; H, 6.11; N, 4.47%. ^1H NMR (CDCl_3) δ 2.442 (3H, s), 2.651 (3H, s), 4.490 (1H, d, $J = 2.4$ Hz, OH), 5.576 (1H, s), 6.600 (1H, d, $J = 7.8$ Hz), 6.681 (1H, d, $J = 7.8$ Hz), 6.98–7.12 (4H, m), 7.150 (1H, d, $J = 2.4$ Hz, NH), 7.371 (2H, m), 7.715

(2H, m). ^{13}C NMR (CDCl_3) δ 18.83 (1C, p), 21.25 (1C, p), 50.16 (1C, t), 75.39 (1C, q), 122.50 (2C, t), 123.27 (2C, t), 124.95 (2C, t), 125.30 (2C, t), 126.83 (1C, t), 129.01 (1C, t), 129.15 (1C, q), 129.40 (1C, q), 141.36 (1C, q), 144.71 (2C, q), 144.81 (2C, q), 145.18 (1C, q).

***N*-(1,4-Dimethyl-9-triptycyl)-*O*-methylhydroxylamine (2).**

To an ice-cold solution of 0.20 g (0.64 mmol) of **11** in 40 mL of diethyl ether was added under argon 0.20 g (1.8 mmol) of KO^tBu suspended in 30 mL of diethyl ether and the mixture was stirred for 15 min at 0 °C. To this mixture was then added dropwise 0.50 mL (8.0 mmol) of methyl iodide and the mixture was stirred for 1.5 h at 0 °C and then for 2 h at room temperature. After quenching with water, the mixture was extracted with diethyl ether. The ether layer was washed with water and brine, dried over MgSO_4 , and evaporated. The residue was recrystallized from dichloromethane–hexane (1:3) to give 0.18 g (0.55 mmol, 86%) of **2**, mp 224–225 °C (dec). Found: C, 84.31; H, 6.45; N, 4.17%. Calcd for $\text{C}_{23}\text{H}_{21}\text{NO}$: C, 84.37; H, 6.46; N, 4.28%. ^1H NMR (CDCl_3) δ 2.435 (3H, s), 2.648 (3H, s), 3.992 (3H, s), 5.554 (1H, s), 6.584 (1H, d, $J = 7.8$ Hz), 6.670 (1H, d, $J = 7.8$ Hz), 6.95–7.10 (4H, m), 7.143 (1H, br s, NH), 7.348 (2H, d, $J = 7.2$ Hz), 7.664 (2H, d, $J = 7.5$ Hz). ^1H NMR (CDCl_3 , –64 °C) δ 2.469 (3H, s), 2.672 (3H, s), 4.044 (3H, s), 5.624 (1H, s), 6.625 (1H, d, $J = 7.7$ Hz), 6.719 (1H, d, $J = 7.7$ Hz), 7.04–7.18 (4H, m), 7.316 (1H, br s, NH), 7.40–7.45 (2H, m), 7.640 (1H, br d, $J = 7.4$ Hz), 7.811 (1H, br d, $J = 7.3$ Hz). ^{13}C NMR (CDCl_3) δ 18.83 (1C, p), 21.46 (1C, p), 50.11 (1C, t), 61.75 (1C, p), 74.82 (1C, q), 122.72 (2C, t), 123.02 (2C, t), 124.91 (2C, t), 125.19 (2C, t), 126.79 (1C, t), 128.98 (1C, t), 129.11 (1C, q), 129.63 (1C, q), 141.42 (1C, q), 144.45 (3C, q), 144.97 (2C, q).

***N*-(1,4-Dimethyl-9-triptycyl)-*O*-ethylhydroxylamine (3).** To an ice-cold solution of 0.50 g (1.6 mmol) of **11** in 40 mL of diethyl ether was added under argon 0.50 g (4.5 mmol) of KO^tBu suspended in 30 mL of diethyl ether and after 15 min 1.0 mL (12.0 mmol) of ethyl iodide. The mixture was stirred for 1.5 h at 0 °C and then for 2 h at room temperature. After quenching with

water, the mixture was extracted with diethyl ether. The ether layer was washed with water and brine, dried over MgSO_4 , and evaporated. The residue was recrystallized from dichloromethane–hexane (1:3) to give 0.42 g (1.23 mmol, 77%) of **3**, mp 117–118 °C. Found: C, 84.50; H, 6.70; N, 4.06%. Calcd for $\text{C}_{24}\text{H}_{23}\text{NO}$: C, 84.42; H, 6.79; N, 4.10%. ^1H NMR (CDCl_3) δ 1.412 (3H, t, $J = 7.0$ Hz), 2.436 (3H, s), 2.656 (3H, s), 4.253 (2H, q, $J = 7.0$ Hz), 5.555 (1H, s), 6.586 (1H, d, $J = 7.8$ Hz), 6.668 (1H, d, $J = 7.8$ Hz), 7.001 (2H, td, $J = 7.2$ and 1.3 Hz), 7.066 (2H, td, $J = 7.3$ and 1.5 Hz), 7.097 (1H, s, NH), 7.346 (2H, dd, $J = 7.3$ and 1.1 Hz), 7.683 (2H, d, $J = 7.2$ Hz). ^1H NMR (CDCl_3 , -64 °C) δ 1.433 (3H, t, $J = 7.0$ Hz), 2.469 (3H, s), 2.678 (3H, s), 4.273 (1H, dq, $J = 9.3$ and 7.0 Hz), 4.343 (1H, dq, $J = 9.3$ and 7.0 Hz), 5.622 (1H, s), 6.625 (1H, d, $J = 7.8$ Hz), 6.720 (1H, d, $J = 7.8$ Hz), 7.06–7.17 (4H, m), 7.251 (1H, br s, NH), 7.417 (2H, d, $J = 7.2$ Hz), 7.622 (1H, d, $J = 7.0$ Hz), 7.848 (1H, d, $J = 7.1$ Hz). ^{13}C NMR (CDCl_3) δ 14.21 (1C, p), 18.82 (1C, p), 21.52 (1C, p), 50.14 (1C, t), 69.37 (1C, s), 74.70 (1C, q), 122.88 (2C, t), 122.99 (2C, t), 124.90 (2C, t), 125.14 (2C, t), 126.77 (1C, t), 129.01 (1C, t), 129.09 (1C, q), 129.66 (1C, q), 141.58 (1C, q), 144.50 (2C, q), 145.00 (1C, q), 145.09 (2C, q).

***N*-(1,4-Dimethyl-9-triptycyl)-*N*-methylhydroxylamine (4).**

To an ice-cold solution of 313 mg (1.0 mmol) of **11** in 30 mL of dichloromethane under argon was added 1.38 g (10 mmol) of potassium carbonate and then 1.10 mL (10 mmol) of methyl trifluoromethanesulfonate. The mixture was stirred for 1.5 h at 0 °C and for 2 h at room temperature, and then heated under reflux for 24 h. The mixture was washed successively with water and brine, and dried over MgSO_4 . Column chromatography on silica gel with benzene as the eluent, followed by recrystallization from dichloromethane–hexane (2:3), gave 110 mg (0.34 mmol, 34%) of **4**, mp 200–201 °C. Found: C, 84.49; H, 6.50; N, 4.22%. Calcd for $\text{C}_{23}\text{H}_{21}\text{NO}$: C, 84.37; H, 6.46; N, 4.28%. ^1H NMR (CDCl_3) δ 2.413 (3H, s), 2.822 (3H, s), 3.715 (3H, s), 5.504 (1H, s), 5.939 (1H, s, OH), 6.630 (1H, d, $J = 8.0$ Hz), 6.645 (1H, d, $J = 8.0$ Hz), 6.90–7.10 (4H, m), 7.33 (1H, dd, $J = 7.2$ and 1.5 Hz), 7.45 (1H, m), 7.57 (1H, br), 8.15 (1H, br). ^1H NMR (CDCl_3 , -62 °C) showed the presence of two isomers in a ratio of 87:13; the major isomer: δ 2.430 (3H, s), 2.902 (3H, s), 3.752 (3H, s), 5.577 (1H, s), 6.188 (1H, s, OH), 6.681 (2H, s), 6.97–7.20 (4H, m), 7.370 (1H, dd, $J = 7.1$ and 1.2 Hz), 7.470 (1H, d, $J = 7.1$ Hz), 7.541 (1H, m), 8.276 (1H, m); the minor isomer: δ 2.485 (3H, s), 2.653 (3H, s), 3.664 (3H, s), 5.545 (1H, s). ^{13}C NMR (CDCl_3 , -62 °C) showed peaks for the major isomer: δ 19.08 (1C, p), 19.10 (1C, p), 47.06 (1C, p), 50.04 (1C, t), 80.42 (1C, q), 123.19 (1C, t), 123.22 (1C, t), 123.52 (1C, t), 124.00 (1C, t), 124.52 (1C, t), 124.54 (1C, t), 125.47 (1C, t), 125.84 (1C, t), 126.78 (1C, t), 128.62 (1C, q), 128.97 (1C, t), 129.33 (1C, q), 141.14 (1C, q), 142.72 (1C, q), 143.76 (2C, q), 145.00 (1C, q), 146.02 (1C, q).

***N*-(1,4-Dimethyl-9-triptycyl)-*N,O*-dimethylhydroxylamine**

(5). To an ice-cold solution of 90 mg (0.28 mmol) of **4** in 6 mL of diethyl ether was added under argon 123 mg (1.1 mmol) of potassium *t*-butoxide suspended in 6 mL of diethyl ether and the mixture was stirred for 15 min. To the mixture was added dropwise 0.31 mL (2.75 mmol) of methyl trifluoromethanesulfonate. This mixture was stirred for 1 h at 0 °C and for 2 h at room temperature, washed successively with aq NaHCO_3 , water, and brine, and dried over MgSO_4 . Recrystallization from ethanol–dichloromethane (1:1) gave 82 mg (0.24 mmol, 87%) of **5**, mp 217–220 °C. Found: C, 84.59; H, 6.75; N, 4.10%. Calcd for $\text{C}_{24}\text{H}_{23}\text{NO}$:

C, 84.42; H, 6.79; N, 4.10%. ^1H NMR (CDCl_3) δ 2.452 (3H, s), 2.661 (3H, s), 3.587 (3H, s), 4.001 (3H, br s), 5.465 (1H, s), 6.639 (1H, d, $J = 7.8$ Hz), 6.694 (1H, d, $J = 7.8$ Hz), 6.88 (1H, br), 6.90–7.10 (3H, m), 7.21 (1H, br), 7.428 (1H, br d, $J = 7.2$ Hz), 7.54 (1H, br), 8.19 (1H, br). ^1H NMR (CDCl_3 , -60 °C) showed the presence of two isomers in a ratio of ca. 95:5; the major isomer: δ 2.490 (3H, s), 2.689 (3H, s), 3.625 (3H, s), 4.049 (3H, s), 5.529 (1H, s), 6.694 (1H, d, $J = 7.8$ Hz), 6.758 (1H, d, $J = 7.8$ Hz), 6.941 (1H, t, $J = 7.2$ Hz), 7.04–7.15 (3H, m), 7.277 (1H, d, $J = 7.2$ Hz), 7.503 (1H, dd, $J = 7.0$ and 1.5 Hz), 7.565 (1H, d, $J = 7.2$ Hz), 8.222 (1H, d, $J = 7.2$ Hz); the minor isomer: δ 2.413 (3H, s), 2.714 (3H, s), 3.603 (3H, s), 3.924 (3H, s), 5.532 (1H, s). ^{13}C NMR (CDCl_3 , -60 °C) showed the peaks for the major isomer: δ 19.01 (1C, p), 21.07 (1C, p), 41.88 (1C, p), 50.29 (1C, t), 59.53 (1C, p), 79.57 (1C, q), 121.98 (1C, t), 122.92 (1C, t), 123.37 (1C, t), 123.91 (1C, t), 124.02 (1C, t), 124.90 (1C, t), 125.46 (1C, t), 126.26 (1C, t), 127.06 (1C, t), 128.32 (1C, q), 128.96 (1C, t), 131.16 (1C, q), 142.23 (1C, q), 142.40 (1C, q), 143.79 (1C, q), 143.91 (1C, q), 145.34 (1C, q), 146.56 (1C, q).

***N*-(1,4-Dimethyl-9-triptycyl)-*O*-ethyl-*N*-methylhydroxylamine (6).**

To an ice-cold solution of 200 mg (0.61 mmol) of **4** in 30 mL of diethyl ether was added under argon 200 mg (1.8 mmol) of potassium *t*-butoxide suspended in 30 mL of diethyl ether and the mixture was stirred for 15 min. To the mixture was added dropwise 0.60 mL (6.7 mmol) of ethyl iodide. The mixture was stirred for 1.5 h at 0 °C and for 2 h at room temperature, washed successively with aq NaHCO_3 , water, and brine, and dried over MgSO_4 . Recrystallization from dichloromethane–hexane (1:1) gave 180 mg (0.51 mmol, 83%) of **6**, mp 143–145 °C. Found: C, 84.73; H, 7.00; N, 4.02%. Calcd for $\text{C}_{25}\text{H}_{25}\text{NO}$: C, 84.47; H, 7.09; N, 3.94%. ^1H NMR (CDCl_3) δ 1.323 (3H, t, $J = 7.2$ Hz), 2.451 (3H, s), 2.673 (3H, br s), 3.592 (3H, br s), 4.20–4.42 (2H, br m), 5.467 (1H, s), 6.640 (1H, d, $J = 7.8$ Hz), 6.693 (1H, d, $J = 7.8$ Hz), 6.88 (1H, br), 6.9–7.1 (3H, m), 7.23 (1H, br), 7.42 (1H, d, $J = 6.6$ Hz), 7.51 (1H, br), 8.22 (1H, br). ^1H NMR (CDCl_3 , -60 °C) showed the presence of two isomers in a ratio of >96:<4; the major isomer: δ 1.350 (3H, t, $J = 7.2$ Hz), 2.490 (3H, s), 2.696 (3H, s), 3.608 (3H, s), 4.282 (1H, dq, $J = 8.4$ and 7.2 Hz), 4.416 (1H, dq, $J = 8.4$ and 7.1 Hz), 5.525 (1H, s), 6.689 (1H, d, $J = 7.8$ Hz), 6.755 (1H, d, $J = 7.8$ Hz), 6.937 (1H, t, $J = 7.4$ Hz), 7.05–7.19 (3H, m), 7.275 (1H, dd, $J = 7.3$ and 1.0 Hz), 7.47–7.53 (2H, m), 8.278 (1H, d, $J = 7.3$ Hz); the minor isomer: δ 1.474 (3H, t, $J = 7.2$ Hz), 2.402 (3H, s), 2.544 (3H, s), 3.011 (3H, s). ^{13}C NMR (CDCl_3 , -63 °C) showed the peaks for the major isomer: δ 13.87 (1C, p), 19.00 (1C, p), 21.07 (1C, p), 42.58 (1C, p), 50.31 (1C, t), 66.92 (1C, s), 79.42 (1C, q), 121.88 (1C, t), 123.00 (1C, t), 123.34 (1C, t), 123.77 (1C, t), 123.98 (1C, t), 124.92 (1C, t), 125.45 (1C, t), 126.23 (1C, t), 127.42 (1C, t), 128.27 (1C, q), 128.94 (1C, t), 131.29 (1C, q), 142.38 (1C, q), 142.59 (1C, q), 143.77 (1C, q), 143.91 (1C, q), 145.34 (1C, q), 146.70 (1C, q).

***N*-(1,4-Dimethyl-9-triptycyl)-*N*-ethyl-*O*-methylhydroxyl-**

amine (7). To a solution of 112 mg (0.34 mmol) of **2** in 40 mL of tetrahydrofuran at -78 °C was added 1.2 mL (81.9 mmol) of butyllithium in hexane (1.56 mol L^{-1}) and the solution was stirred at -78 °C for 15 min. To this solution was added dropwise 0.4 mL (5.0 mmol) of ethyl iodide and the mixture was stirred for 5 h and left to warm up to room temperature. After evaporation of the solvent, the residue was submitted to column chromatography (SiO_2 , benzene–hexane) to give 78 mg (0.22 mmol, 64%) of **7**, mp 167–168 °C (from dichloromethane–hexane). Found: C, 84.45; H,

Table 3. Crystal Data of Compounds 4–7 and Parameters for Data Collection, Structure Determination, and Refinement

Compound	4	5	6	7
Empirical formula	C ₂₃ H ₂₁ NO	C ₂₄ H ₂₃ NO	C ₂₅ H ₂₅ NO	C ₂₅ H ₂₅ NO
Formula weight	327.41	341.43	355.46	355.46
Crystal system	monoclinic	monoclinic	monoclinic	monoclinic
Space group	<i>P</i> 2 ₁ / <i>c</i>	<i>P</i> 2 ₁ / <i>c</i>	<i>P</i> 2 ₁ / <i>c</i>	<i>P</i> 2 ₁ / <i>c</i>
<i>a</i> /Å	9.927(4)	10.336(1)	9.957(2)	9.859(5)
<i>b</i> /Å	17.790(4)	17.161(1)	13.022(2)	18.557(9)
<i>c</i> /Å	10.163(3)	10.543(2)	14.539(1)	10.768(6)
β /°	106.97(2)	104.42(1)	92.047(2)	105.864(6)
<i>V</i> /Å ³	1717.5(9)	1811.2(4)	1883.7(4)	1895(1)
<i>Z</i>	4	4	4	4
<i>D_c</i> /g cm ^{−3}	1.265	1.2521	1.253	1.246
<i>F</i> (000)	696	728	760	760
μ (Mo-K α)/cm ^{−1}	0.71069	0.71069	0.71069	0.7107
Temp/K	293(2)	293(2)	293(2)	100.2
2 θ _{max} /°	55	55	55	54.5
No. of reflections measured				
Total	3937	4161	4285	10699
Unique	2780	2897	2395	4085
No. of refinement variables	317	235	244	245
Final <i>R</i> ; <i>R_w</i>	0.053; 0.144	0.047; 0.126	0.059; 0.156	0.077; 0.144
<i>GOF</i>	1.063	1.103	0.956	1.580

$$R = \Sigma ||F_o| - |F_c|| / \Sigma |F_o|, R_w \text{ on } F^2.$$

7.18; N, 3.93%. Calcd for C₂₅H₂₅NO: C, 84.47; H, 7.09; N, 3.94%. ¹H NMR (CDCl₃) δ 1.681 (3H, br t, *J* = 6.9 Hz), 2.433 (3H, br s), 2.636 (3H, br s), 3.3–4.6 (5H, br), 5.445 (1H, s), 6.55–6.70 (2H, m), 6.75–7.10 (4H, br), 7.1–8.5 (4H, br). ¹H NMR (CDCl₃, −60 °C) showed the presence of two isomers in a ratio of 73:27; the major isomer: δ 1.682 (3H, t, *J* = 7.0 Hz), 2.485 (3H, s), 2.635 (3H, s), 3.471 (1H, dq, *J* = 14.2 and 7.2 Hz), 4.312 (3H, s), 4.448 (1H, dq, *J* = 14.2 and 6.8 Hz), 5.499 (1H, s), 6.678 (1H, d, *J* = 7.8 Hz), 6.744 (1H, d, *J* = 7.8 Hz), 6.928 (1H, td, *J* = 7.4 and 0.8 Hz), 7.03–7.15 (3H, m), 7.265 (1H, dd, *J* = 6.8 and 0.8 Hz), 7.502 (1H, dd, *J* = 6.8 and 1.4 Hz), 7.724 (1H, d, *J* = 7.4 Hz), 8.321 (1H, d, *J* = 7.5 Hz); the minor isomer: δ 1.766 (3H, t, *J* = 7.3 Hz), 2.410 (3H, s), 2.749 (3H, s), 3.677 (1H, dq, *J* = 16.2 and 7.4 Hz), 4.001 (3H, s), 4.262 (1H, dq, *J* = 16.2 and 7.2 Hz), 5.543 (1H, s), 6.662 (2H, s), 7.004 (1H, t, *J* = 7.4 Hz), 7.03–7.15 (4H, m), 7.362 (1H, dd, *J* = 7.0 and 1.2 Hz), 7.480 (1H, dd, *J* = 6.8 and 1.4 Hz), 8.280 (1H, d, *J* = 7.5 Hz). ¹³C NMR (CDCl₃, −63 °C), the major isomer: δ 15.03 (1C, p), 19.02 (1C, p), 21.30 (1C, p), 49.15 (1C, s), 50.41 (1C, t), 67.03 (1C, p), 80.50 (1C, q), 121.50 (1C, t), 123.06 (1C, t), 123.43 (1C, t), 123.74 (1C, t), 123.79 (1C, t), 124.85 (1C, t), 125.41 (1C, t), 126.16 (1C, t), 128.09 (1C, t), 128.18 (1C, q), 128.65 (1C, t), 131.40 (1C, q), 142.15 (1C, q), 143.10 (1C, q), 143.61 (1C, q), 143.68 (1C, q), 145.79 (1C, q), 146.99 (1C, q); the minor isomer: δ 19.17 (1C, p), 19.24 (1C, p), 20.86 (1C, p), 50.16 (1C, t), 50.60 (1C, s), 59.60 (1C, p), 81.17 (1C, q), 122.49 (1C, t), 123.13 (1C, t), 123.23 (1C, t), 123.86 (1C, t), 124.43 (1C, t), 124.50 (1C, t), 125.41 (1C, t), 125.69 (1C, t), 127.77 (1C, t), 128.02 (1C, q), 128.82 (1C, t), 131.81 (1C, q), 142.08 (1C, q), 142.37 (1C, q), 143.89 (1C, q), 144.86 (1C, q), 144.95 (1C, q), 145.54 (1C, q).

***N*-(1,4-Dimethyl-9-triptycyl)-*N*,*O*-diethylhydroxylamine (8).**

To a solution of 150 mg (0.43 mmol) of **2** in 30 mL of tetrahydrofuran at −78 °C was added 1.2 mL (1.9 mmol) of butyllithium in hexane (1.56 mol L^{−1}) and the solution was stirred at −78 °C for 15 min. To this solution was added dropwise 0.4 mL (5.0 mmol)

of ethyl iodide and the mixture was stirred for 5 h and left to warm up to room temperature. After evaporation of the solvent, the residue was subjected to column chromatography (SiO₂, benzene–hexane) to give 123 mg (0.33 mmol, 77%) of **8**, mp 142–143 °C (from dichloromethane–hexane). Found; C, 84.72; H, 7.22; N, 3.73%. Calcd for C₂₆H₂₇NO: C, 84.51; H, 7.36; N, 3.79%. ¹H NMR (CDCl₃) δ 1.258 (3H, br t, *J* = 6.9 Hz), 1.660 (3H, br t, *J* = 6.9 Hz), 2.431 (3H, br s), 2.633 (3H, br s), 3.532 (1H, br), 4.2–4.6 (3H, br), 5.441 (1H, s), 6.60–6.68 (2H, br m), 6.8–8.5 (8H, br m). ¹H NMR (CDCl₃, −60 °C) showed the presence of two isomers in a ratio of 70:30; the major isomer: δ 1.282 (3H, t, *J* = 7.1 Hz), 1.656 (3H, t, *J* = 6.8 Hz), 2.484 (3H, s), 2.638 (3H, s), 3.439 (1H, dq, *J* = 14.3 and 7.3 Hz), 4.33–4.68 (3H, m), 5.501 (1H, s), 6.673 (1H, d, *J* = 7.8 Hz), 6.737 (1H, d, *J* = 7.8 Hz), 6.926 (1H, t, *J* = 7.4 Hz), 6.97–7.17 (3H, m), 7.266 (1H, d, *J* = 7.1 Hz), 7.506 (1H, d, *J* = 7.1 Hz), 7.682 (1H, d, *J* = 7.5 Hz), 8.410 (1H, d, *J* = 7.5 Hz); the minor isomer: δ 1.335 (3H, t, *J* = 7.1 Hz), 1.746 (3H, t, *J* = 7.0 Hz), 2.403 (3H, s), 2.729 (3H, s), 3.658 (1H, dq, *J* = 16.1 and 7.1 Hz), 4.137 (1H, quint, *J* = 7.4 Hz), 4.248 (1H, dq, *J* = 16.1 and 7.1 Hz), 4.33–4.68 (1H, m), 5.537 (1H, s), 6.661 (2H, s), 6.97–7.17 (4H, m), 7.359 (1H, d, *J* = 7.0 Hz), 7.479 (1H, d, *J* = 7.1 Hz), 7.520 (1H, d, *J* = 7.1 Hz), 8.345 (1H, d, *J* = 7.2 Hz). ¹³C NMR (CDCl₃, −63 °C), the major isomer: δ 14.48 (1C, p), 15.27 (1C, p), 19.01 (1C, p), 21.34 (1C, p), 49.18 (1C, s), 50.39 (1C, t), 72.79 (1C, s), 80.50 (1C, q), 121.46 (1C, t), 123.08 (1C, t), 123.18 (1C, t), 123.37 (1C, t), 123.62 (1C, t), 124.72 (1C, t), 125.37 (1C, t), 126.06 (1C, t), 128.10 (1C, q), 128.57 (1C, t), 128.64 (1C, t), 131.52 (1C, q), 142.34 (1C, q), 143.38 (1C, q), 143.51 (1C, q), 143.69 (1C, q), 145.78 (1C, q), 147.01 (1C, q); the minor isomer: δ 14.30 (1C, p), 19.13 (1C, p), 19.23 (1C, p), 19.56 (1C, p), 50.15 (1C, t), 51.07 (1C, s), 65.68 (1C, s), 81.09 (1C, q), 122.54 (1C, t), 123.62 (2C, t), 123.87 (1C, t), 124.35 (1C, t), 124.42 (1C, t), 125.41 (1C, t), 125.51 (1C, t), 128.02 (1C, t), 128.07 (1C, q), 128.81 (1C, t), 131.81 (1C, q), 142.02

Table 4. Kinetic Data for Stereomutation^{a)}

Compd	Process ^{b)}	Obsd protons	Temp range ^{c)} °C	Pts ^{c)}	ΔH^\ddagger	ΔS^\ddagger
					kJ mol ⁻¹	J mol ⁻¹ K ⁻¹
2	E	8,13-H	-35 to -11	6	50.1 ± 3.3	-9.0 ± 13.1
3	E	8,13-H	-29 to -1	6	49.5 ± 6.2	-11.6 ± 23.6
		CH ₂	-41 to -16	5	49.0 ± 4.0	-13.1 ± 16.4
4	D	1-CH ₃	-50 to -23	6	49.1 ± 0.8 ^{d)}	-16.4 ± 3.3 ^{d)}
					49.0 ± 0.7 ^{e)}	-2.6 ± 3.1 ^{e)}
		8,13-H ^{f)}	80 to 117	5	73.9 ± 8.5	-8.7 ± 23.1
5	E	8,13-H ^{f)}	76 to 100	5	66.7 ± 10.8	-12.0 ± 30.5
6	E	8,13-H ^{f)}	71 to 101	5	68.8 ± 13.6	-9.1 ± 37.8
7	D	1-CH ₃	-14 to 6	5	60.8 ± 2.9 ^{d)}	11.8 ± 10.8 ^{d)}
					61.0 ± 1.5 ^{e)}	4.5 ± 5.7 ^{e)}
		CH ₂	37 to 57	6	60.9 ± 2.2	-12.0 ± 6.9
8	D	1-CH ₃	-22 to -1	5	57.8 ± 4.4 ^{d)}	8.1 ± 16.7 ^{d)}
					57.7 ± 4.5 ^{e)}	0.9 ± 17.1 ^{e)}

a) Measured in CDCl₃ unless otherwise stated. b) E and D denote enantiomerization and diastereomerization, respectively. c) The temperature range and points used in the lineshape analysis. d) $R^*(-sc)^* \rightarrow R^*-ap$. e) $R^*-ap \rightarrow R^*(-sc)^*$. Rate constants for the reverse process are calculated from those for the forward process and the corresponding equilibrium constants. Conformer populations are given in Table 2. f) Measured in toluene-*d*₈.

(1C, q), 142.43 (1C, q), 143.79 (1C, q), 144.86 (1C, q), 145.10 (1C, q), 145.61 (1C, q).

X-ray Crystallography. Crystals of compounds **4–7** grown from dichloromethane–hexane were used. The crystal data and the parameters for data collection, structure determination, and refinement are summarized in Table 3. Diffraction data were collected on a Rigaku AFC7R or a Rigaku/MSM Mercury CCD diffractometer and calculations were performed using the SHELXL97 program.⁹ The structures were solved by direct methods followed by full-matrix least-squares refinement with all non-hydrogen atoms anisotropic and hydrogen atoms isotropic. Reflection data with $|I| > 2.0\sigma(I)$ were used for **4–6** and those with $|I| > 3.0\sigma(I)$ for **7**. The function minimized was $\sum w(|F_o| - |F_c|)^2$ where $w = [\sigma^2(F_o)]^{-1}$.

Crystallographic data of compounds **4–7** have been deposited at the CCDC, 12 Union Road, Cambridge, CB2 1EZ, UK and copies can be obtained on request, free of charge, by quoting the publication citation and the deposition numbers 212008–21211, respectively.

Lineshape Analysis. Total lineshape analysis was performed by visual matching of experimental spectra with theoretical spectra computed on an NEC PC9821Xs personal computer equipped with a Mutoh PP-210 plotter using the DNMR3K program, a modified version of the DNMR3 program¹⁰ converted for use on personal computers by Dr. Hiroshi Kihara. Temperature dependences of chemical shift differences, T_2 values, and conformer populations were properly taken into account. The analysis of the diastereomerization processes was made using the 1-methyl signals because the chemical shift differences between the conformers were the largest. In the analysis of the enantiomerization processes, the peri-proton (8/13H) signals were used for compounds **2–6** and the methylene signals for compounds **3** and **7**; the results from the two probes agreed well in **3**. It was assumed that the diastereomerization takes place too fast to affect the lineshape in the temperature range for the enantiomerization analysis.

The enthalpies and entropies of activation obtained by the least-squares analysis of the Eyring plots are compiled in Table 4 together with the temperature ranges and the temperature points used in the lineshape analysis.

References

- 1 G. Yamamoto, F. Nakajo, N. Endo, and Y. Mazaki, *Bull. Chem. Soc. Jpn.*, **74**, 1467 (2001).
- 2 G. Yamamoto, C. Agawa, and M. Minoura, *Bull. Chem. Soc. Jpn.*, **76**, 825 (2003).
- 3 C. F. Wilcox, Jr. and E. N. Farley, *J. Am. Chem. Soc.*, **106**, 7195 (1984); S. Gronowitz and G. Hansen, *Ark. Kemi*, **27**, 145 (1967).
- 4 a) M. Raban and D. Kost, in "Acyclic Organonitrogen Stereodynamics," ed by J. B. Lambert and Y. Takeuchi, VCH Publishers, New York (1992), Chap. 2. b) F. G. Riddell, *Tetrahedron*, **37**, 849 (1981). c) M. Raban and D. Kost, *Tetrahedron*, **40**, 3345 (1984).
- 5 For the nomenclature for absolute conformations, see: W. Klyne and V. Prelog, *Experientia*, **16**, 521 (1960); M. Ōki, *Top. Stereochem.*, **14**, 1 (1983).
- 6 Y. Tanaka, G. Yamamoto, and M. Ōki, *Bull. Chem. Soc. Jpn.*, **56**, 3023 (1983); Y. Tanaka, M. Sc. Dissertation, The University of Tokyo (1982).
- 7 Since the conformer assignments in **12** and **13** were based solely on the ¹H NMR chemical shifts in Ref. 6, we performed NOE experiments on these compounds and confirmed that the previous assignments were correct.
- 8 See for example: G. Bott, L. D. Field, and S. Sternhell, *J. Am. Chem. Soc.*, **102**, 5618 (1980).
- 9 G. M. Sheldrick, Program for the Refinement of Crystal Structures, University of Göttingen, Germany (1997).
- 10 D. A. Kleier and G. Binsch, QCPE Program No. 165.